



Reducing of UV Radiation Intensity, Ozone Concentration and Fume Formation in Gas Metal Arc Welding

V. I. Vishnyakov¹ · S. A. Kiro¹ · A. A. Ennan¹

Received: 1 April 2020 / Revised: 26 May 2020 / Accepted: 9 June 2020 / Published online: 8 July 2020
© Institute of Earth Environment, Chinese Academy Sciences 2020

Abstract

The UV radiation intensity and mass concentration of ozone in air are studied experimentally in the gas metal arc welding. Effects of the shielding gas composition influence on UV radiation intensity, ozone concentration and welding fume formation are demonstrated. Addition of potassium via wetting the electrode wire or work-piece by aqueous solution of potassium carbonate and via its premix with shielding gas leads to decrease of UV radiation and ozone formation during arc welding. Discussions of the observed effects and theoretical model of radiation absorption are presented.

Keywords Gas metal arc welding · Welding fumes · Ultraviolet · Ozone · Potassium additional agent

1 Introduction

The welding arc emit high levels of ultraviolet (UV) radiation, and its exposure significantly increases the risk of skin and ocular hazards for welders and related workers (Emmett et al. 1981; Dixon and Dixon 2004). Arc UV radiation intensity depends on the welding method (the maximum UV is observed when the shielding inert gas is used) and the welding parameters: arc current and voltage, shielding gas composition and flow rate, type of base metal and wire (Dennis et al. 1997; Ioffe et al. 1997; Okuno 1987; Okuno et al. 2001; Peng et al. 2007). Change of any of these parameters during the welding process results in UV radiation variation.

The UV radiation with wavelengths less than 240 nm causes the generation of toxic gas ozone (O₃) (Lunau 1967; Liu et al. 2007). Therefore, the ozone concentration should be correlated with the radiation intensity in range UV-C (200–280 nm), and varies with the distance from the arc. Technological opportunities for reducing ozone concentration in the welder's breathing zone by choosing the optimal welding conditions (minimum intensity of UV-C radiation) are limited, because the possible changes in weldability and weld quality should be taken into account.

Dennis et al. (2002) proposed small amount of reducing gas NO or CH₄ to the argon shielding gas. The ozone concentration is significantly decreased because of chemical reaction with these reducing gases. However, it occurs only in the region where the shielding gas mixes with the surrounding air (near arc). It is known that in wavelengths of UV-C range the absorption of radiation in air is relatively low and ozone can be created at long distance from the arc. Thus, outside the mixing region, UV radiation from welding arc produces ozone as before.

Because the primary mechanism of ozone formation in welding operations is UV radiation, it is necessary to decrease the UV-C intensity from the arc. This can be done via addition of substances with a low ionization potential in the welding process.

Potassium additive to the shielding gas CO₂ was studied by Vishnyakov et al. (2017). The effect of potassium additional agent on the fume formation was demonstrated, because low ionization potential of potassium (4.3 eV) causes the change in plasma composition: the iron ions (iron ionization potential is 7.9 eV) are replaced by potassium ions with higher number density. However, low ionization potential of potassium should provide the absorption of UV radiation with photon energy $h\nu \geq 4.3$ eV, which corresponds to the wavelength $\lambda \leq 288$ nm. Accordingly, ozone formation should be decreased when potassium is added in the welding process.

The present paper is devoted to measurements of the UV radiation intensity and ozone content in air in gas metal arc

✉ V. I. Vishnyakov
eksvar@ukr.net; dr.v.vishnyakov@gmail.com

¹ Physical-Chemical Institute for Environment and Human Protection, 3 Preobrazhenska st, Odessa, UA 65082, Ukraine

welding (GMAW) with different compositions of shielding gas and different contents of potassium additional agent, which is added on the surface of electrode wire or work-piece, or into the shielding gas.

2 Experimental equipment and technique

The scheme of experimental equipment is presented in Fig. 1. The electrode wire ER 70S-6 and ER-308 with diameter 0.8 mm was used for bead-on-plate welding on rotatable flat disk with thickness 10 mm and diameter 220 mm under stationary torch inside the fume chamber. The weld disk material is low-carbon steel St3 or stainless steel AISI 304.

The DC MMA/TIG/MIG/MAG Paton PSI-250R inverter rectifier was used as a source of reverse polarity (when electrode wire is positive and molten pool is negative) direct current of 90 ± 5 A and voltage of 23 V. The welding torch was fixed in a single position with distance between contact tube and weld disk of 15 mm and the angle between it and wire axis was 90° . The exhaust hood was mounted on the distance 25 cm from the weld disk for prevention of welding fumes accumulation. Wire feed speed was 10 cm/s and welding speed was 6.5 mm/s. Shielding gas flow rate was 12 l/min.

The UV radiometer-dosimeter Tenzor-71 (Research and Production Company “Tenzor”, Ukraine) was used for UV radiation intensity determination. Three spectral intervals

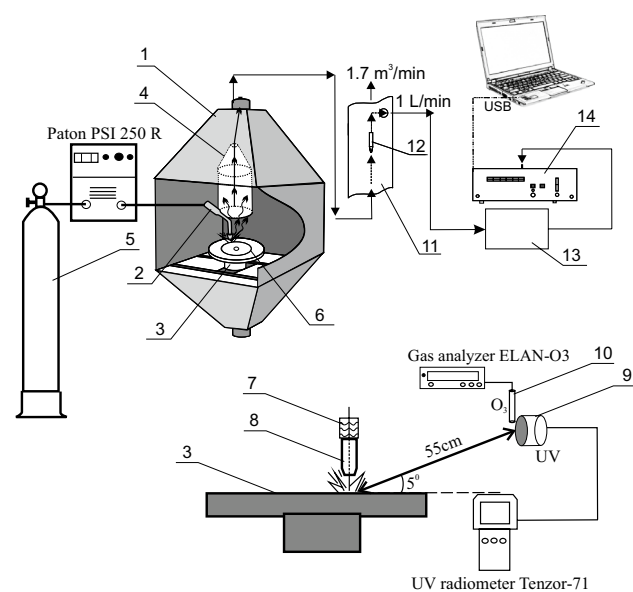


Fig. 1 Scheme of experimental equipment: 1, fume chamber; 2, welding torch; 3, turntable; 4, exhaust hood; 5, shielding gas bottle; 6, weld bead; 7, dish with cotton wool; 8, welding torch nozzle; 9, UV detector; 10, air sampler; 11, vertical pipe; 12, nozzle for isokinetic sampling; 13, dual-stage aerosol dilution system; 14, laser aerosol spectrometer

were studied: 315–400 nm (UV-A), 280–315 nm (UV-B) and 200–280 nm (UV-C). Calibrated detector was located on the fixed distance of 55 cm from arc, in the direction of 5° angel to the weld disk surface.

Measurements were made within 30 s during welding process with step of 1 s. The samples of measured values are presented in Fig. 2 for the pure argon as a shielding gas, ER-308 as an electrode wire and stainless steel AISI 304 as a material of weld disk. The deviations of measured values are caused by welding arc instability.

The gas analyzer with electrochemical detector ELAN-O₃ (NPO “ECO-INTECH”, Russia) was used for the measurement of ozone mass concentration in air with relative error 20%. The glass tip with fluoropolymer tubing (which are resistant to ozone and UV radiation) was used as an air sampler with flow rate of 0.3 l/min. The air sampler also was located on the distance of 55 cm from arc, near UV-detector.

The particle number in the sample of welding fume was measured using the laser aerosol spectrometer LAS-P (Model 9814.290.000, Karpov Institute of Physical Chemistry, Moscow, Russia). The LAS-P aerosol spectrometer allows determination of particles’ size distribution ranging from 0.15 to 1.5 μ m in the media characterized by particle concentrations up to $2 \times 10^3/\text{cm}^3$. The maximum relative errors in determining the volume of the air samples and the size of particles and their number density were 5% and 10% respectively. The multichannel size distribution had the following size ranges (μm): 0.15–0.2; 0.2–0.25; 0.25–0.3; 0.3–0.4; 0.4–0.5; 0.5–0.7; 0.7–1.0; 1.0–1.5; > 1.5.

The particle number density in the sample had the typical value of $10^5/\text{cm}^3$. Therefore, the dual-stage aerosol dilution

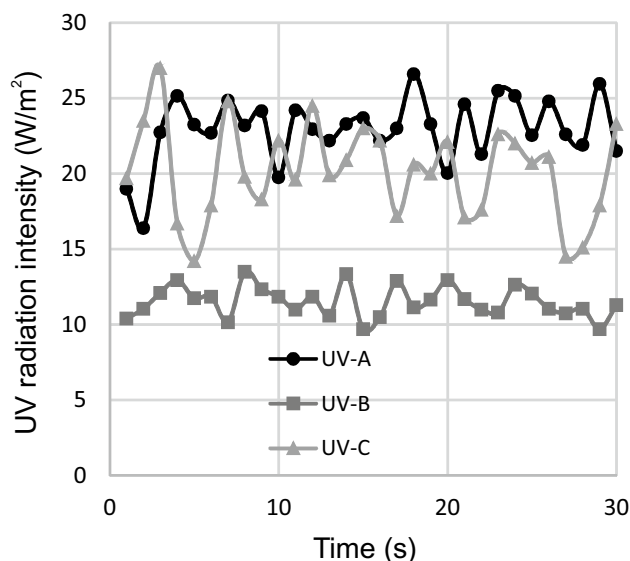


Fig. 2 Sample of the UV radiation intensity measurements; the shielding gas is pure argon

system with the total dilution ratio of 230 for sample flow rate 1 Lpm was used. Petryanov's filters with the collection efficiency of at least 99.99% for the particles with size of $0.15 - 0.2 \mu\text{m}$ were used in the dilution system.

Potassium additional agent was used in welding process. Potassium injection into the arc zone was carried out in three different ways:

1. The aqueous solution of potassium carbonate was applied onto the electrode wire by its wetting. The dish with cotton wool, moistened by solution, was located over the contact tube, and electrode wire was trailed through the cotton wool. Mass flow rate of potassium was determined by measuring the dish weight changes over the welding time and the wire feed speed.
2. The aqueous solution of potassium carbonate was uniformly applied onto the predicted surface area of the weld bead, and the rotatable flat disk was dried before welding. The calculation of the potassium mass flow rate during welding was based on the welding speed, weld bead surface area and solution concentration.
3. Potassium injection into shielding gas was carried out using pneumatic nebulizer. This method is described in detail by Vishnyakov et al. (2017).

3 Measurement results

The dependency of UV radiation intensity on the shielding gas composition was observed earlier by Dennis et al. (1997) and Nakashima et al. (2016). Presented in Fig. 3a measurement results confirm these observations. The electrode wire ER 308, the arc current 95 A for pure argon and for mixture Ar with 8% CO_2 ; and current 85 A for pure CO_2 were used.

The ozone formation is effected by UV radiation of wavelength less than 240 nm ($h\nu \sim 5 \text{ eV}$), i.e. in the UV-C range. Accordingly, ozone concentration also depends on the shielding gas composition. The results of ozone mass concentration measurements are presented in Fig. 3b.

Effect of potassium additional agent on the radiation intensity in UV-C range is demonstrated in Fig. 4a. In this case, potassium was inlet in the arc plasma via wetting the electrode wire by aqueous solution of potassium carbonate. The arc current 95 A and the pure argon as shielding gas were used. The dependency of ozone mass concentration, under same conditions, is presented in Fig. 4b.

Effect of potassium additional agent on the radiation intensity in UV-C range, when the weld disk is wetted by aqueous solution of potassium carbonate, is demonstrated in Fig. 5a. The arc current 95 A and the pure argon as shielding gas were used. The dependency of ozone mass concentration, under same conditions, is presented in Fig. 5b.

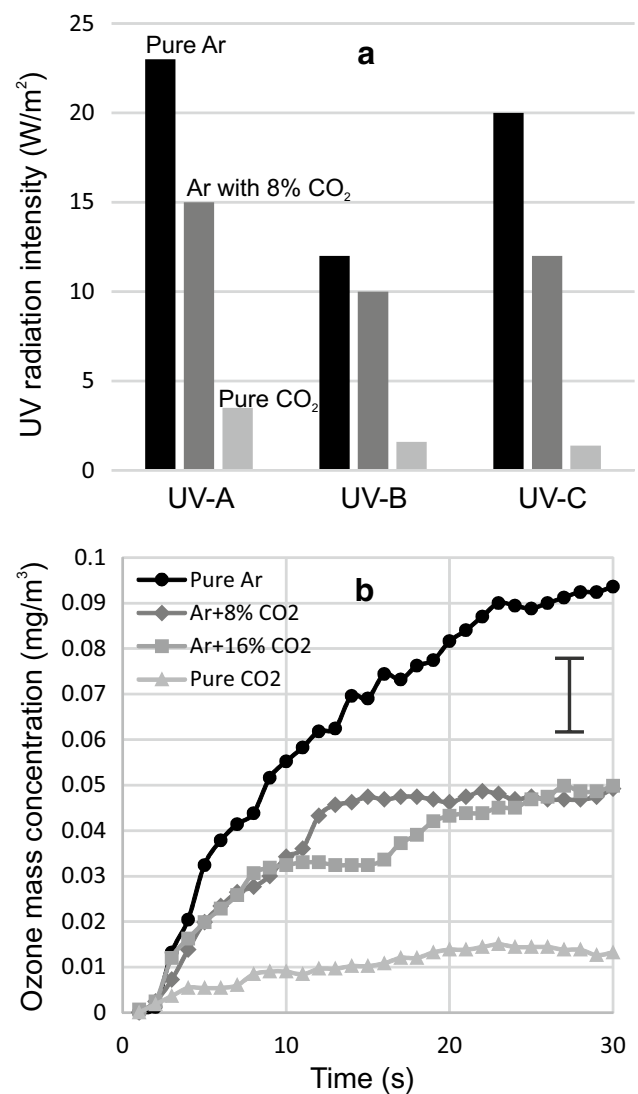


Fig. 3 UV radiation intensity from GMAW with different compositions of shielding gas (a) and evolution of ozone content in air for the different shielding gases (b)

Effect of potassium additional agent on the radiation intensity in UV-C range, when potassium is premixed with shielding gas, is demonstrated in Fig. 6a. The arc current 95 A and the pure argon as shielding gas were used. The dependency of ozone mass concentration, under same conditions, is presented in Fig. 6b.

It should be noted that addition of potassium into the shielding gas requires the increase of potassium rate; because potassium is premixed with shielding gas and its number density is distributed more uniformly around arc column. The influences of electrode wire (ER 70S-6 or ER-308) and weld disk materials (low-carbon steel St3 or stainless steel AISI 304), and weld speed (in range of 5.5–7.5 mm/s) are negligible: difference in the measured values are less than error limit. It does not mean that such

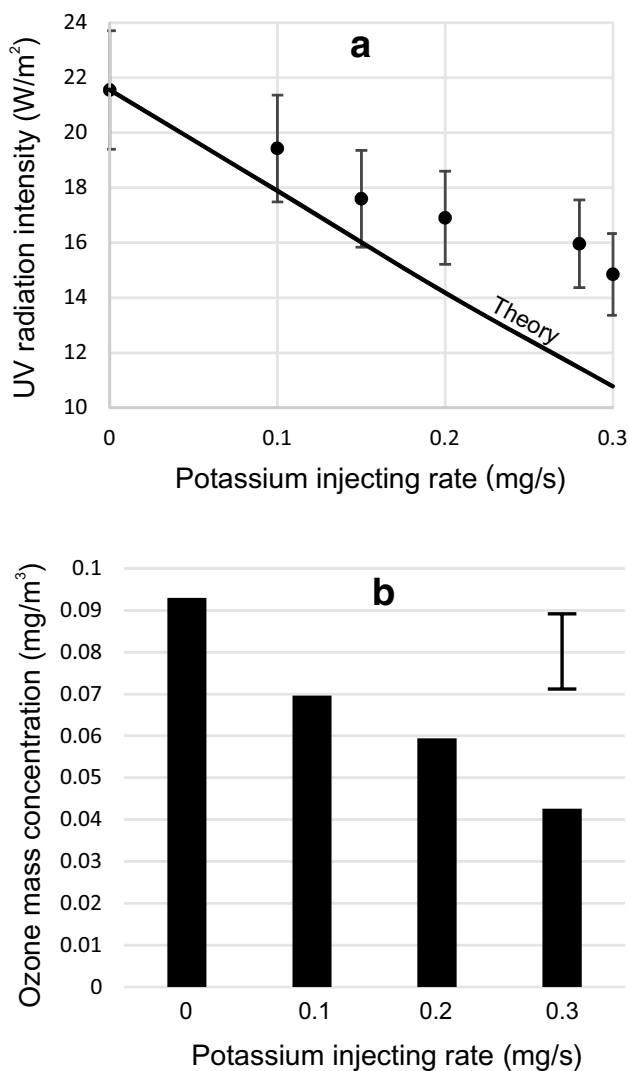


Fig. 4 Dependencies of UV-C radiation intensity (a) and ozone mass concentration (b) on the potassium injecting mass rate on the electrode wire; the shielding gas is pure argon

dependencies are absent at all (for example, see Okuno (1985), where steel and aluminum are considered), but these problems are outside of consideration in present paper.

Presence of potassium in the shielding gas also effects on the welding fume formation rate, which occurs as a result of condensation of the ionized metal vapors. Without potassium the iron ions play the role of condensation centers. Potassium atoms have low ionization potential ($I_K = 4.3 \text{ eV}$, $I_{Fe} = 7.9 \text{ eV}$), therefore provide greater ion number density, which become the condensation centers. This causes the decrease of nucleus number density and, accordingly, the decrease of inhalable particle number density in the breathing zone. The nucleation in the welding fumes is described in Ref. Vishnyakov et al. (2019-2).

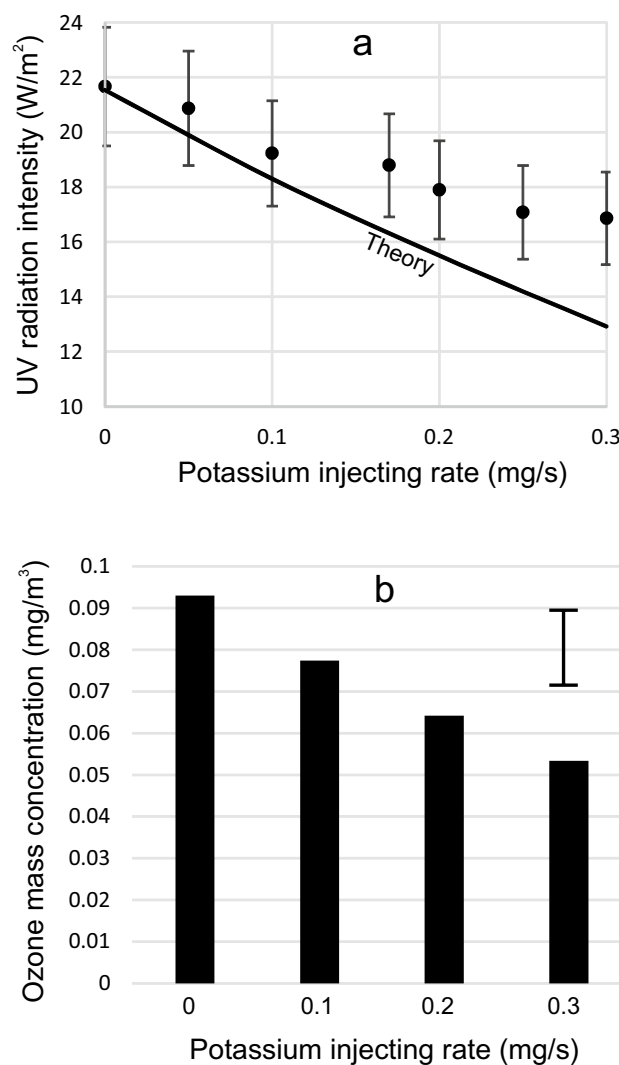


Fig. 5 Dependencies of UV-C radiation intensity (a) and ozone mass concentration (b) on the potassium injecting mass rate on the work-piece; the shielding gas is pure argon

Inhalable particles have the bimodal size distribution. Dependencies of the measured particle number densities for these two modes on the potassium number density, injected by wetting of electrode wire, are presented in Fig. 7.

The particle number density decreases at the low potassium injecting rates and remains constant with increase of this rate. It is caused by the ionization mechanism change while potassium injecting. Without potassium the ionization balance in welding fume is determined by ionization of iron atoms on the surface of nuclei. The addition of potassium leads to replacing of the surface ionization by volumetric impact ionization (Vishnyakov et al. 2019-2), which occurs already at the low potassium number density.

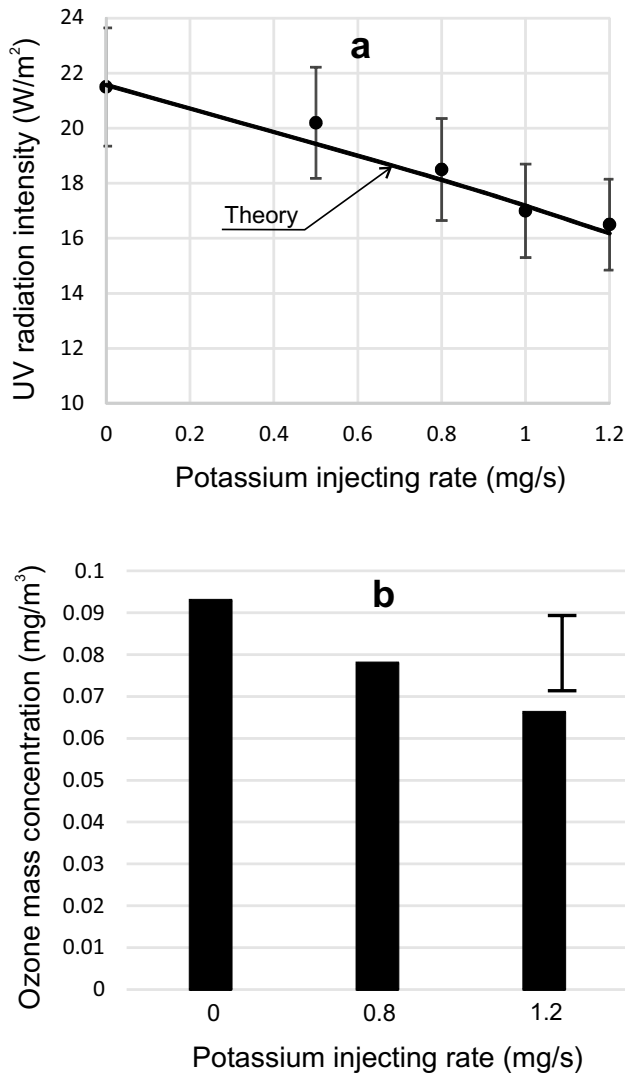


Fig. 6 Dependencies of UV-C radiation intensity (**a**) and ozone mass concentration (**b**) on the potassium injecting mass rate in the shielding gas; the shielding gas is pure argon

4 Discussion

The welding arc UV radiation in the range of 120–240 nm is produced, mostly, by recombination of the shielding gas ions (Ioffe et al. 1997). Recombination radiation exists because of recombination collisions of free electrons and ions resulting in the neutral atoms formation. The intensity of such radiation is proportional to the degree of plasma ionization squared. The spectrum of recombination radiation is composed of lines and continuum. The energy of photon, which is emitted when the electron collides and recombines with an ion, is equal to the sum of kinetic energy and the binding energy of the recombined electron. Since the kinetic energy of the electron is not quantized, this forms a continuous spectrum with lines at the binding energy of the levels.

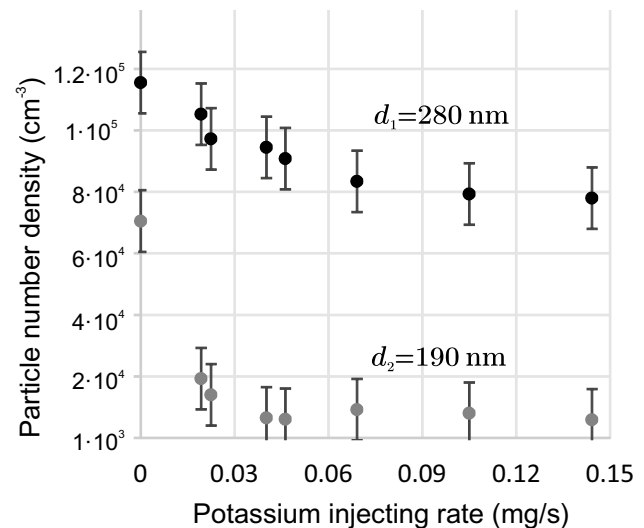


Fig. 7 Particle number densities in the welding fume for modes with average diameter $d_1 = 280$ nm and average diameter $d_2 = 190$ nm

The measured radiation intensity in UV-C range is ~ 20 W/m² on the distance 55 cm from arc, when pure argon as shielding gas is used. Measurements showed the inversely square dependency of the intensity on the distance from arc, i.e. arc can be described as a point source of radiation. Planck's law determines the radiation intensity of continuous spectrum:

$$R_{\text{ph}} = \frac{2\pi(k_B T_{\text{eff}})^4}{c^2 h^3} \int_{x_1}^{x_2} \frac{x^3}{\exp x - 1} dx, \quad (1)$$

where k_B is the Boltzmann constant; T_{eff} is the effective temperature of the radiation source; c is the light velocity; h is the Planck constant. The values of limits $X_{1,2} = hv_{1,2}/k_B T_{\text{eff}}$ are determined by measured range of radiation: for UV-C range $hv_1 = 4.4$ eV and $hv_2 = 6.2$ eV.

Equation (1) gives measured intensity of radiation (20 W/m²) on the distance 55 cm from arc for effective temperature $T_{\text{eff}} = 8000$ K. Accordingly, the photon flux in range UV-C is $j_{\text{ph}} = 2.5 \times 10^{21}$ /cm²s on the boundary of arc column and $j_{\text{ph}} = 7 \times 10^{15}$ /cm²s on the distance 55 cm from arc.

The presence of atoms with low ionization potential in shield layer around arc can provide the absorption of UV radiation, which generates ozone. One of such materials is a potassium with ionization potential $I_K = 4.3$ eV.

The potassium vapor from electrode wire or molten pool is mixed with metal vapors and shielding gas, and extends outside of the arc column. The aura around arc column is visually observed when potassium is added. The potassium injection into arc plasma by evaporation from the welding wire can be

described, in simple approach, as a point source in the laminar flow of shielding gas (Socolofsky and Jirka 2002):

$$v_{sg} \frac{\partial n_K}{\partial z} = D_K \left[\frac{1}{r} \frac{\partial}{\partial r} \left(r \frac{\partial n_K}{\partial r} \right) + \frac{\partial^2 n_K}{\partial z^2} \right], \tag{2}$$

where $v_{sg} = 4J_{sg}/\pi d_{torch}^2$ is the shielding gas velocity, $J_{sg} = 12$ l/min is the shielding gas flow rate, $d_{torch} = 15$ mm is the welding torch inner diameter; n_K is the potassium atom number density; D_K is the potassium diffusivity; z is the coordinate directed from electrode wire to molten pool; r is the radius vector across arc column ($r^2 = x^2 + y^2$). The boundary conditions are

$$n_K = 0, \quad r, z \rightarrow \infty, \\ -4\pi r^2 m_{aK} D_K \nabla n_K = J_{mK}, \quad r = \frac{d_w}{2}, z = 0,$$

where m_{aK} is the potassium atom mass, J_{mK} is the potassium evaporation mass rate (0.1, 0.2 and 0.3 mg/s), $d_w = 0.8$ mm is the electrode wire diameter.

Solution of Eq. (2) is

$$n_K(z, r) = \frac{J_{mK}}{4\pi m_{aK} D_K \sqrt{r^2 + z^2}} \times \exp \left[-\frac{v_{sg}}{2D_K} \left(\sqrt{r^2 + z^2} - z \right) \right]. \tag{3}$$

Potassium diffusivity

$$D_K = \frac{1}{3} \lambda_{aK} \sqrt{\frac{8k_B T_{arc}}{\pi m_{aK}}} \sim 10 \frac{\text{cm}^2}{\text{s}},$$

where $\lambda_{aK} \sim 1 \mu\text{m}$ is the mean free path of potassium atoms; $T_{arc} \sim 15,000$ K (Khrabry et al. 2018) is the arc temperature for arc current density $\sim 10^7$ A/m². Layer of potassium, which absorbs the UV radiation is located around the arc column, which average diameter is 3 mm. The arc column boundary has the average distance $r_b = 1.5$ mm from arc axis. The distributions of potassium number density along arc in the thin layers at the distance of 1.5 mm and 4 mm from arc axis are presented in Fig. 8 for the different potassium injecting mass rate.

It should be noted, that diffusivity outside arc region differs from it inside and depends on the distance from arc axis, because the temperature of shielding gas changes as

$$T(r) = T_{sg} + (T_b - T_{sg}) \exp \frac{r_b - r}{l_{mix}}, \tag{4}$$

where $T_{sg} = 300$ K is the initial temperature of shielding gas; $T_b = 3000$ K is the temperature of welding fumes on the arc column boundary; l_{mix} is the mixing length, which is determined experimentally (Vishnyakov et al. 2018), and in the system under consideration $l_{mix} \sim 10$ mm.

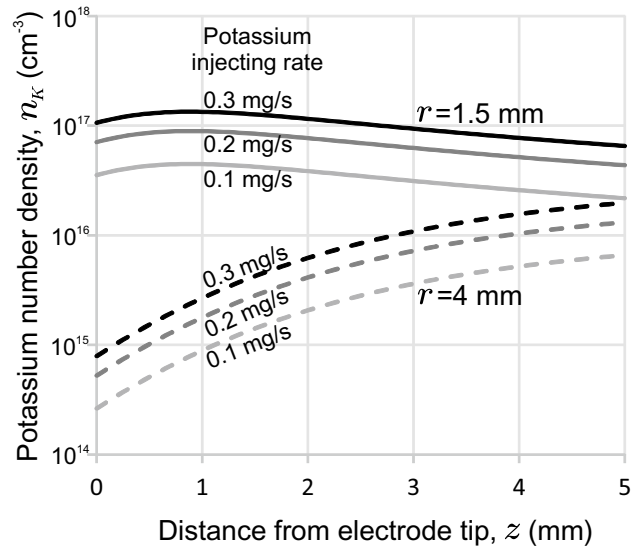


Fig. 8 Potassium number density in the thin layer at the distance of 1.5 mm and 4 mm from arc axis

The average value of potassium number density along arc column is

$$n_{rmavK}(r) = \frac{1}{l_{arc}} \int_0^{l_{arc}} n_K(z, r) dz, \tag{5}$$

where $l_{arc} \sim 6$ mm is the arc length.

The photoionization rate of potassium in UV-C range can be determined in Kramers-Heisenberg approach (YaB and Raizer 1966; Vishnyakov et al. 2019-1) by the following equation:

$$\left. \frac{dn_{e(i)}}{dt} \right|_{ph} = \frac{n_a 16I_K^3}{3\sqrt{3}\pi^2 c^3 e^2 m_e^2} \times \int_{X_K}^{x_2} \frac{dx}{x(\exp x - 1)} = \frac{n_a}{\tau_{UV}}, \tag{6}$$

where n_e , n_i and n_a is the electron, ion and atom number densities respectively, and $n_a = n_{avK} - n_i$; e is the absolute value of electron charge; m_e is the electron mass; $X_K = I_K/k_B T_{eff}$, $\tau_{UV} \sim 10 \mu\text{s}$ is the photoionization relaxation time.

Thus, photoionization rate, which provides the photon absorption, directly depends on the ionizable atom number density; and it should be considered that atom ionization occurs not only by photoionization.

Ionization rate via electron-atom collisions is described as

$$\left. \frac{dn_{e(i)}}{dt} \right|_{\text{col}} = n_e n_a k_{\text{ion}}, \tag{7}$$

where $k_{\text{ion}} = \pi r_{\text{aK}}^2 v_{\text{Te}}$ is the ionization rate constant (Mitchner and Kruger 1973); r_{aK} is the potassium atom radius; $v_{\text{Te}} = \sqrt{8k_{\text{B}}T/\pi m_e}$ is the electron thermal velocity.

The relaxation time for impact ionization on the arc column boundary $(n_e k_{\text{ion}})^{-1} \sim 0.02 \mu\text{s}$, that is much less than photoionization relaxation time in the system under consideration. The photoionization performs weak effect on the ionization balance, which, therefore, can be determined by Saha equation (Kittel 1969):

$$\frac{n_e n_i}{n_a} = \frac{\sum_e v_e \exp \frac{-I_K}{k_{\text{B}}T}}{\sum_i} \equiv K_S, \tag{8}$$

where \sum_i and \sum_a are the statistical weights for ions and atoms respectively; $v_e = 2(2\pi m_e k_{\text{B}}T/h^2)^{3/2}$ is the electron states' effective density; K_S is the Saha constant. Condition of neutrality is

$$n_e = n_i = n_0, \tag{9}$$

where n_0 is the unperturbed number density, which depends on the distance from arc axis, because temperature and potassium initial number density n_{avK} are changed with r ,

$$n_0(r) = \frac{K_S(r)}{2} \left(\sqrt{1 + 4 \frac{n_{\text{avK}}(r)}{K_S(r)}} - 1 \right), \tag{10}$$

and, accordingly, atom number density, which is used in Eq. (6), can be defined as $n_a = n_{\text{avK}} - n_0$.

The photoionization rate Eq. (6) describes the production of electrons (ions) and, accordingly, extinction of photons:

$$\begin{aligned} \left. \frac{dn_{e(i)}}{dt} \right|_{\text{ph}} &= \frac{n_{\text{avK}}(r) - n_0(r)}{\tau_{\text{UV}}} \\ &= - \frac{dn_{\text{ph}}}{dt} = - \frac{dj_{\text{ph}}}{dr}. \end{aligned} \tag{11}$$

Therefore, the photon flux, which is absorbed by potassium via photoionization is

$$j_{\text{ph}}^*(r) = \int_{r_b}^r \frac{n_{\text{avK}}(r) - n_0(r)}{\tau_{\text{UV}}} dr, \tag{12}$$

and radiation intensity after absorption in the gas layer with potassium is

$$R_{\text{ph}}^*(r) = R_{\text{ph}} \frac{j_{\text{ph}} - j_{\text{ph}}^*(r)}{j_{\text{ph}}}. \tag{13}$$

The attenuation of radiation intensity in UV-C range via absorption by potassium $R_{\text{ph}}^*(r)/R_{\text{ph}}$ is presented in Fig. 9a. The basic absorption of radiation occurs in the layer with thickness of 4 mm, where local potassium number density has a high value.

The attenuation of radiation intensity when potassium evaporates from the molten pool is described similarly. However, premixing potassium with shielding gas provides the spatial distribution of potassium atom number density

$$n_{\text{K}}^{\text{sg}}(r) = \frac{J_{\text{mK}}}{J_{\text{msg}}} \frac{P}{k_{\text{B}}T(r)}, \tag{14}$$

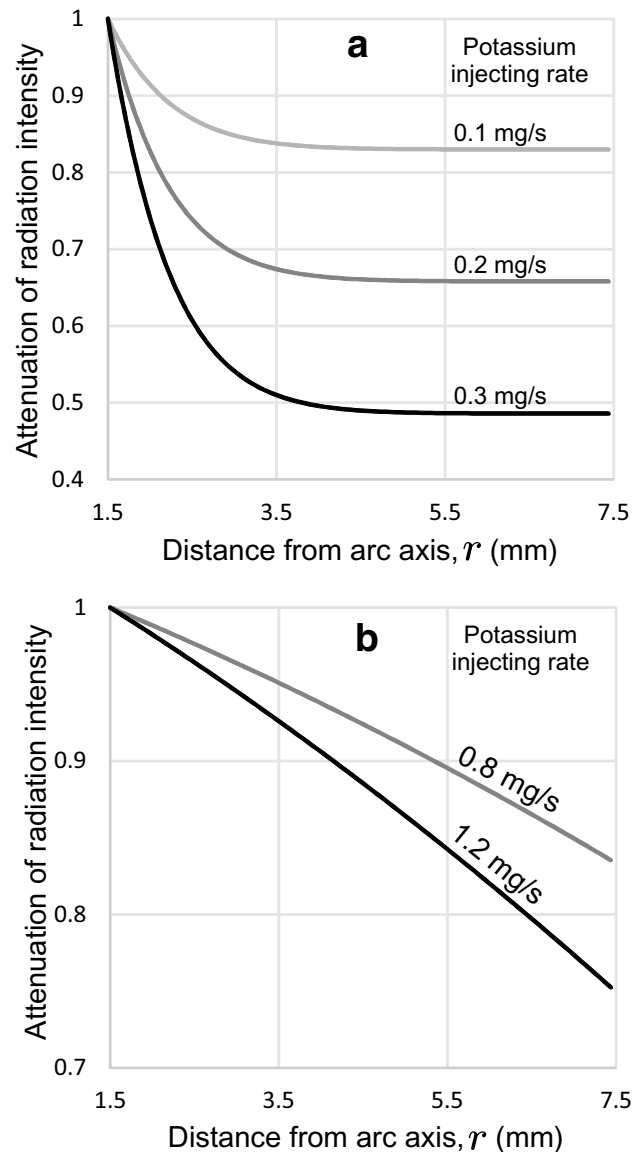


Fig. 9 Dependencies of radiation attenuation on the thickness of absorbing layer for different potassium injecting rates on the electrode wire (a) and in the shielding gas (b)

where J_{mK} is the potassium mass flow rate (0.8 and 1.2 mg/s); $J_{msg} = 350$ mg/s is the shielding gas mass flow rate; P is the atmospheric pressure; $T(r)$ is the gas temperature in layer (4). The radiation attenuation in this case is described as

$$\frac{R_{ph}^*(r)}{R_{ph}} = 1 - \frac{1}{j_{ph}\tau_{UV}} \int_{r_b}^r [n_K^{sg}(r) - n_0(r)] dr, \quad (15)$$

and is presented in Fig. 9b. It is taken into account that n_0 in Eq. (15) is determined by n_K^{sg} .

In this case, the potassium is distributed more uniformly in the gas layer with smaller number density and greater potassium injecting rate is necessary for considerable absorption of the UV radiation.

The comparisons of experimental data with theoretical results are presented in Figs. 4, 5, 6. For injecting of potassium via evaporation (Figs. 4 and 5), theory yields stronger potassium influence than experiment, though the global trend is identical. This is explained by simplicity of theoretical model, where diffusion of potassium in the laminar flow of shielding gas is used. In real systems the flow turbulence should be considered. For premixing of potassium with shielding gas, theory describes the experimental data quite well (Fig. 6).

5 Conclusion

The measurements of UV radiation intensity and ozone mass concentration in air when gas metal arc welding was used, demonstrated the attenuation of both intensity of radiation in UV-C range, and ozone concentration under potassium additional agent in the welding process.

Potassium injection into the arc zone was carried out in three different ways: via wetting the electrode wire or welding disk by aqueous solution of potassium carbonate, or by premix of the droplets of such a solution with shielding gas. Two first techniques demonstrated more effective attenuation of the radiation and ozone concentration.

Theoretical analysis demonstrated that using the wetting of electrode wire provides the high local potassium number density in the welding fume near arc column boundary; and basic absorption of radiation occurs in the layer with thickness of 4 mm. The premix of potassium with shielding gas leads to its more uniform distribution in the gas layer around arc column with smaller local number density and provides weaker radiation absorption.

The addition of potassium in the welding process leads to decrease of the particle number density in welding fumes, because presence of potassium provides the volumetric impact ionization of its atoms.

Thus, it can be recommended to add the potassium into covering of the welding wire for decrease of hazard from UV radiation and ozone formation in the welding process.

References

- Dennis JH, Mortazavi SB, French MJ, Hewitt PJ, Redding CR (1997) The effects of welding parameters on ultraviolet light emissions, ozone and Cr^{VI} formation in MIG welding. *Ann Occup Hyg* 41:95–104
- Dennis JH, French MJ, Hewitt PJ, Mortazavi SB, Redding CAJ (2002) Control of exposure to hexavalent chromium and ozone in gas metal arc welding of stainless steels by use of a secondary shield gas. *Ann Occup Hyg* 46:43–48
- Dixon AJ, Dixon BF (2004) Ultraviolet radiation from welding and possible risk of skin and ocular malignancy. *Med J Aust* 181:155–157
- Emmett EA, Buncher CR, Suskind RB, Rowe KWJr (1981) Skin and eye diseases among arc welders and those exposed to welding operations. *J Occup Med* 23:85–90
- Ioffe I, Koss V, Perelman N, Hilton D (1997) UV radiation of the GTA welding plasma versus shielding gas composition. *J Phys D Appl Phys* 30:793–797
- Khrabry A, Kaganovich I, Nemchinsky V, Khodak A (2018) Investigation of the short argon arc with hot anode. I. Numerical simulation of non-equilibrium effects in the near-electrode region. *Phys Plasmas* 25:013521
- Kittel C (1969) *Thermal physics*. Wiley, New York
- Liu HH, Wu YC, Chen HL (2007) Production of ozone and reactive oxygen species after welding. *Arch Environ Contam Toxicol* 53:513–518
- Lunau FW (1967) Ozone in arc welding. *Ann Occup Hyg* 10:175–188
- Mitchner M, Kruger CH (1973) *Partially ionized gases*. Wiley, New York
- Nakashima H, Utsunomiya A, Takahashi J, Fujii N, Okuno T (2016) Hazard of ultraviolet radiation emitted in gas metal arc welding of mild steel. *J Occup Health* 58:452–459
- Okuno T (1985) Spectra of optical radiation from welding arcs. *Ind Health* 23:53–70
- Okuno T (1987) Measurement of ultraviolet radiation from welding arcs. *Ind Health* 25:147–156
- Okuno T, Ojima J, Sayto H (2001) Ultraviolet radiation emitted by CO₂ arc welding. *Ann Occup Hyg* 45:597–601
- Peng C, Liu H, Chang C, Shieh J, Lan C (2007) Evaluation and monitoring of UVR in shield metal arc welding processing. *Health Phys* 93:101–108
- Socolofsky SA, Jirka GH (2002) *Environmental fluid mechanics part I. Lecture notes, Institute for Hydromechanics, University of Karlsruhe, Germany, Mass Transfer and Diffusion*
- Vishnyakov VI, Kiro SA, Oprya MV, Shvets OI, Ennan AA (2017) Nonequilibrium ionization of welding fume plasmas; effect of potassium additional agent on the particle formation. *J Aerosol Sci* 113:178–188
- Vishnyakov VI, Kiro SA, Oprya MV, Chursina OD, Ennan AA (2018) Numerical and experimental study of the fume chemical composition in gas metal arc welding. *Aerosol Sci Eng* 2:109–117
- Vishnyakov VI, Kozytskyi SV, Ennan AA (2019a) Change of ionization mechanism in the welding fume plasma from gas metal arc welding. *Aerosol Sci Eng* 3:49–53
- Vishnyakov VI, Kozytskyi SV, Ennan AA (2019b) Features of nucleation in welding fumes from gas metal arc welding. *J Aerosol Sci* 137:105439
- YaB Zel'dovich, Raizer YuP (1966) *Physics of shock waves and high-temperature hydrodynamic phenomena, vol 1*. Academic, New York